

# Proximal surrogate measures for proactive safety evaluation of right-angle vehicle collisions in an intersection

Patrick Marvin G. Agramon<sup>1</sup>, Ma. Bernadeth B. Lim<sup>2\*</sup>, Mark Joel B. Uaje<sup>3</sup>, Harvey S. Maunahan<sup>4</sup>

<sup>1</sup> Bachelor of Science in Civil Engineering Graduate, Department of Civil Engineering, College of Engineering and Agro-Industrial Technology, University of the Philippines Los Baños, Laguna, Philippines

<sup>2</sup> Assistant Professor, Department of Civil Engineering, College of Engineering and Agro-Industrial Technology, University of the Philippines Los Baños, Laguna, Philippines

<sup>3,4</sup> Instructor, Department of Civil Engineering, College of Engineering and Agro-Industrial Technology, University of the Philippines Los Baños, Laguna, Philippines

Correspondence: [mblim4@up.edu.ph](mailto:mblim4@up.edu.ph)

## ABSTRACT

As road traffic accidents, injuries, and deaths have been persistent throughout the years, the demand for road safety development has increased. This study focuses on developing proactive safety evaluations of unsignalized intersections by using the proximal surrogate measure of Post-Encroachment Time (PET) in measuring the risk of transverse collisions. Procedures involved the determination of peak hour period, manual measurement of PET, identification of critical conflict zones, and development of prediction models for crash estimations. A total of 1551 conflicts were observed, in which an average PET value of 3.57s was obtained. The PET dataset was subjected to goodness-of-fit tests, and the best-fitting model of Johnson SU distribution was determined. Through this statistical model, the probability of right-angle collisions was determined to be 18.11%. Subsequently, it was estimated that 793 crashes per year are predicted to occur within the intersection. The determination of intersection safety levels was unfeasible due to the lack of relative safety standards for this procedure. However, the study has provided safety parameters that can be used as references in evaluating risk mitigation policies and safety projects for the intersection.

**Keywords:** road safety, unsignalized T-junction, intersection accident analysis, post-encroachment time

## INTRODUCTION

In a report by the World Health Organization (2018), the number of road traffic deaths has increased to 1.35 million global cases in 2016. Moreover, the statistical trend for the number of road crashes in Metro Manila is also on the rise (MMDA 2019). Traditional methods of on-road safety evaluation involve the use of historical accident data which pose longer and more difficult approaches in the process of safety evaluation. Additionally, these types of evaluations lean toward

reactive approaches which depend on the premise that accidents must have occurred first before road safety could be evaluated (Killi and Vedagiri 2014). In tackling these growing challenges to road safety, it is more desirable to use faster and more efficient methods that are independent of using historical accident data in the road safety analysis.

Traffic conflict technique (TCT) is one of the developing methods in establishing proactive road safety analysis. This technique was developed from the concept of analyzing traffic conflicts or critical incidents that denote near-collision occurrences (Chin and Quek 1997). Traffic conflict is best described as the reactive evasive response of two or more vehicles due to a near-collision event (Parker and Zegeer 1989). Research interest in the proactive surrogate approach in quantifying the severity and risks of traffic conflicts has gained popularity over the years (Mahmud et al. 2016). This approach uses surrogate safety measures or observable events within a traffic conflict that can assume highly probable collisions or instances of “almost accidents”, near-misses, traffic conflicts, etc. (Varhelyi et al. 2018). These measures attribute several variables such as distance, deceleration, and other indicators for vehicle conflict (Mahmud et al. 2016). The following are listed surrogate measures for safety evaluation: Time to Collision (TTC), Time Exposed Time to Collision (TET), Time Integrated Time to Collision (TIT), Modified TTC (MTTC), Crash Index (CI), Time-to-Accident (TA), Time Headway (H), and PET (Mahmud et al. 2016). PET is the time difference between the last transverse vehicle entry time and first vehicle exit time at a certain node. According to Pirdavani et al. (2010), PET is one of the most commonly used surrogate measures in evaluating intersections, as it is easier to extract and analyze than of general parameters such as TTC.

In a study by Kili and Vedagiri (2014), surrogate safety measures were used in evaluating an unsignalized three-legged intersection, for which they obtained frequency distributions of

vehicle PET that allowed the identification of intersection nodes with the highest conflict frequencies. Their follow-up study in 2016 has developed this methodology by using the concept of critical speeds, which led them to obtain conflict distributions of different types of turning vehicles and evaluate a three-legged intersection into having 20.3% total right-angle or transverse conflicts. On the other hand, Songchitruska (2004) conducted an innovative non-crash-based safety evaluation of intersections using the extreme value theory approach. A total of 18 four-legged intersections were considered in their study, in which PET values were determined through automated, semi-automated, and manual methods of counting. It was found that the manual method of PET determination produced the lowest percentage of measurement error and was subsequently used for the study. Additionally, the validity of PET as a safety indicator was also tested in Songchitruska's study, in which historical crash data were used as response variables for Poisson and Negative Binomial Regression methods for PET validation. After establishing the validity of PET for safety evaluation, the extreme value theory approach was made possible and consequently produced annual crash frequency models for 18 intersections in Lafayette, Indiana. Multiple studies on the extreme value theory approach for the analysis of proximal surrogate measures have then been prominent in the field of road safety research (Farah and Azevedo 2016; Pawar et al. 2018; Goyani et al. 2019; Reddy et al. 2019). This growing literature on proximal surrogate measures has continuously paved developments in road safety analysis; however, Zheng et al. (2014) assert that difficulties in cross-validations and generalizations still inhibit major developments in this field.

This study intends to apply and broaden knowledge on the use of proximal safety analysis. It aims to proactively evaluate the road safety performance of an unsignalized T-junction without dependence on historical data. It specifically aims to evaluate the frequency of right-angle conflicts

at a T-junction using the proximal surrogate measure of PET, determine critical conflict zones for transverse collisions within the intersection, develop and calibrate statistical models for crash frequency estimations, and estimate the probability of right-angle collisions within the intersection. The study can help in providing a quicker approach to obtaining road safety information, which could then evaluate the effectiveness of related road safety policies. The application of this study to the selected intersection can help the local traffic offices in obtaining reference data for developing intersection safety policies.

## **METHODS**

The methodology consists of four major parts, namely: site selection, data collection, data extraction and processing, and safety analysis.

### **Site Selection**

Selected study area is San Pabo City, a component city in the landlocked province of Laguna, Philippines. The land area of the city is about 197 square kilometers which constitutes 10.25% of Laguna's total area. According to the 2020 Census the population of the city is around 285,348. This represented 8.44% of the total population of Laguna province. The population density is 1,444 inhabitants per square kilometer (PhilAtlas, 2023). The city has a growing population and economic activities, hence becoming more congested during peak hours, weekends and holidays.

In determining specific intersection for the study, the following guidelines on site selection according to the literature recommendations were set also considering available traffic footage provided by the San Pablo City Traffic Management Office (SPCTMO):

- The intersection must be multi-laned and three-legged.
- The intersection must be unsignalized.

- The intersection must be equipped with surveillance equipment that provides a clear perspective over the intersection for traffic data collection.
- The intersection must be continuously operating.
- Instances of right-angle collisions are feasibly observable by the surveillance equipment.

The study site of Rizal Avenue-Holy Rosary Street T-Junction was selected based on the aforementioned site characteristics. It is an unsignalized three-legged intersection or T-junction that is located at the entry point of Barangay Bagong Pook, San Pablo City, Laguna. It connects the local road of Holy Rosary street to Rizal Avenue, which serves as a collector road for vehicles entering and exiting the city proper. Rizal Avenue operates as a major road with four lanes, in which two lanes are dedicated to each opposing traffic. Its northbound traffic leads to the Colago-Cosico Avenue intersection, while the southbound traffic leads to the San Pablo City Plaza or the city proper of San Pablo itself. Holy Rosary street, on the other hand, is a two-lane minor road that serves as the main entry point to Barangay Bagong Pook. Moreover, the junction in the study is relatively close to the non-operating San Pablo-Malvar Philippine National Railway (PNR) railroad track. The intersection is equipped with pavement markings, pedestrian lanes, railroad crossing signage, and CCTV footages at video frame rate of 30 fps. Commercial establishments near the intersection include gas stations, a Utility Van (UV) – express terminal, and a few convenience stores. Figures 1 and 2 show the location of the intersection in both plan and street views, respectively.

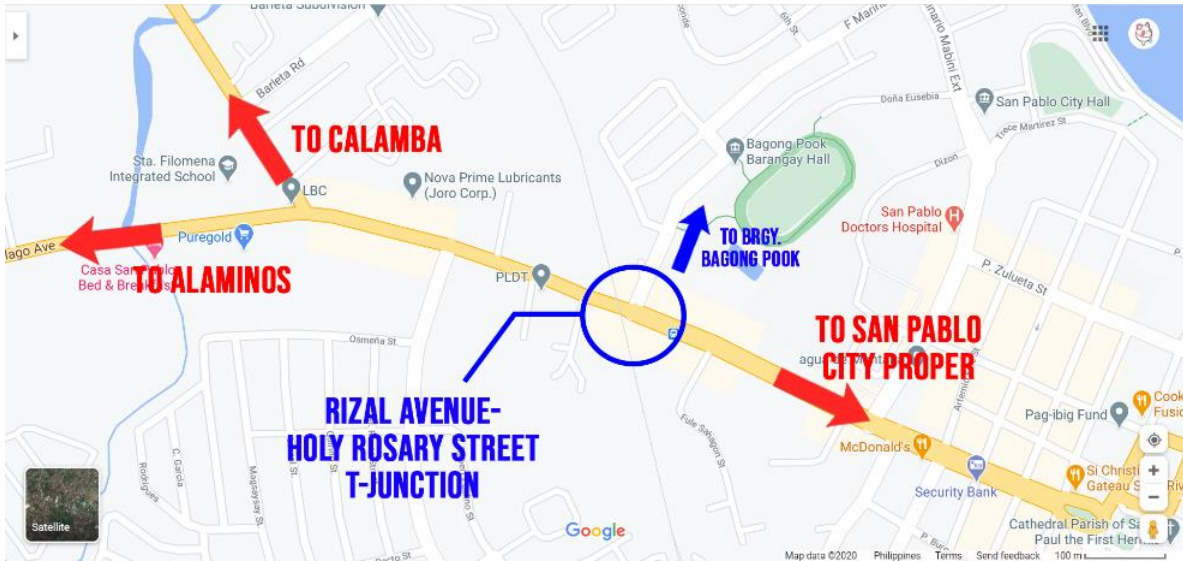


Figure 1. Rizal Avenue-Holy Rosary Street T-Junction Plan View.



Figure 2. Rizal Avenue-Holy Rosary Street T-Junction Street View.

### Traffic Data

Traffic data to be analyzed for this study is collected through a road inventory survey and classified traffic volume count. Figure 3 presents the study intersection sketch, in which geometric

properties and road facilities are shown. The sketch shows that the road widths of the major and minor roads are 10.4 m and 4.5 m, respectively.

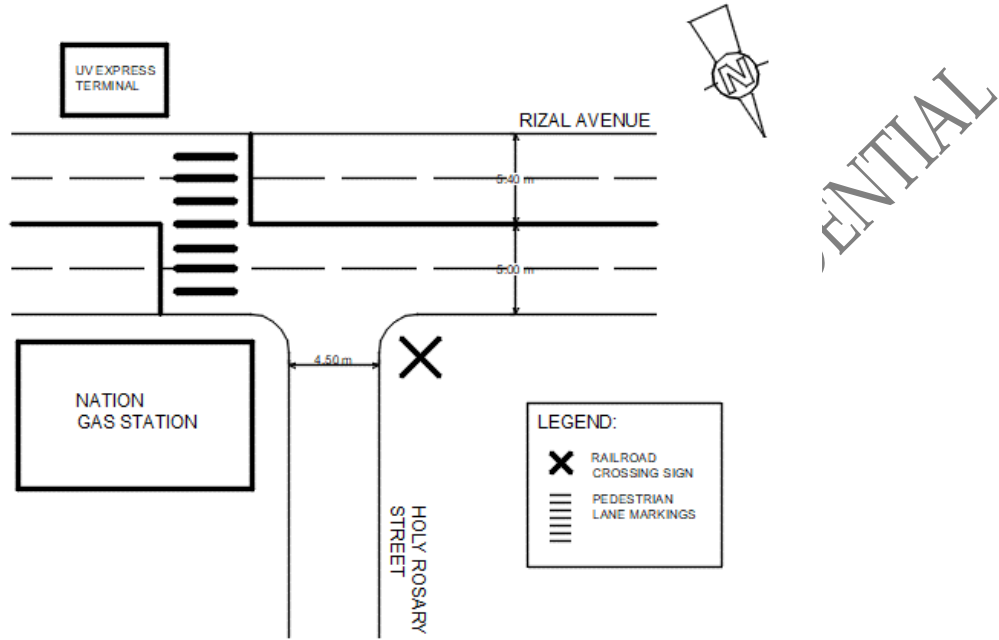


Figure 3. Study Intersection Sketch.

A classified traffic volume count was done during peak hour period (10-11 AM) to estimate the traffic condition and vehicular composition of the intersection in this study. Each vehicle movement was given designations and is presented in Figure 4. All directional movements as shown in the figure (V1-V13) were considered to feasibly obtain critical conflict zones for right-angle collisions. A total of 60 forms have been processed and were encoded in Microsoft Excel for analysis.



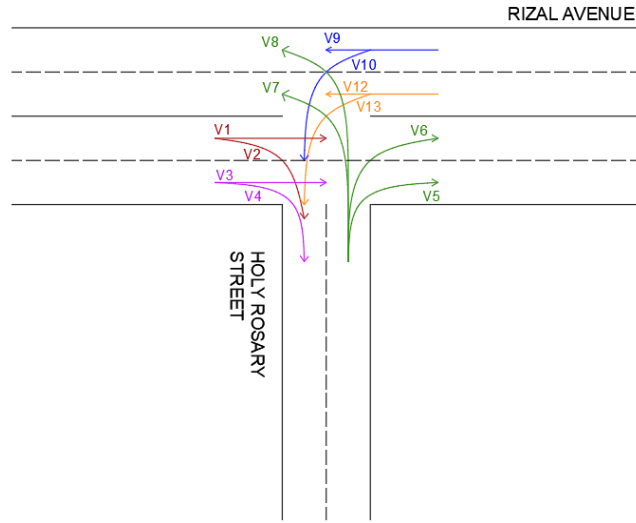


Figure 4. Plan view of the observed vehicle movements in the T-junction.

Figures 5 and 6 show the 15-minute traffic volume variations at 6 to 11 AM and 3 to 8 PM, respectively. The variation charts show that the traffic volume peaked at the period of 10:00 to 11:00 AM, which has a total flowrate of 5581 pcu/hr.

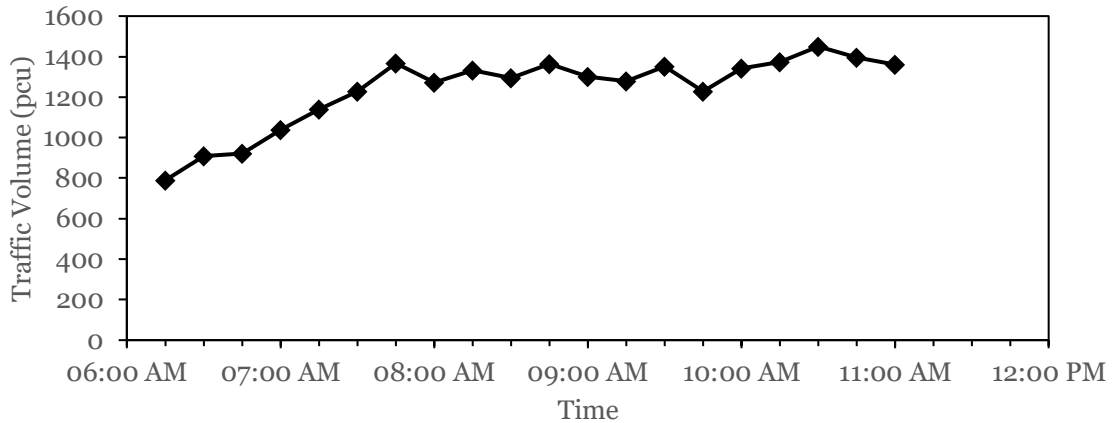


Figure 5. 15-minute Traffic Volume Variation from 6 to 11 AM.

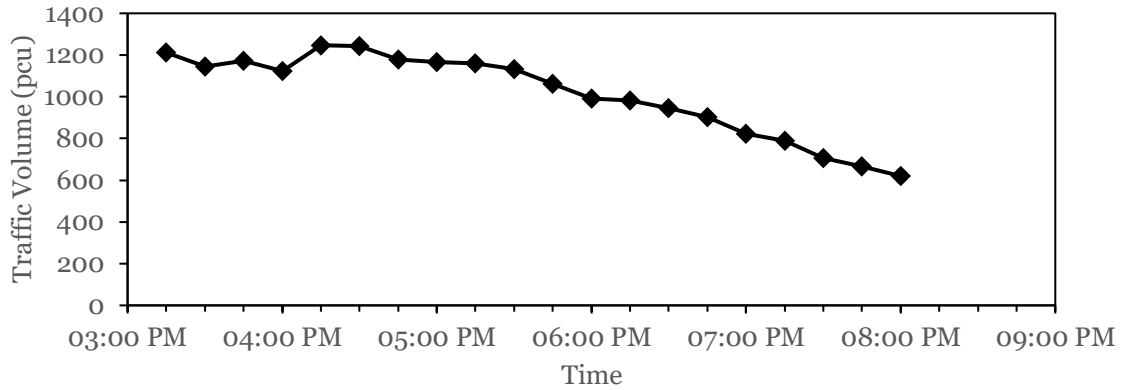


Figure 6. 15-minute Traffic Volume Variation from 3 to 8 PM.

The traffic volume count for each vehicle classification in the traffic flow is summarized in Figure 7. It was found that the traffic flow is mostly composed of three-wheelers (3W), covering 57% of the overall traffic composition. It could be observed that the traffic composition was greatly affected by the IATF regulations, in which PUJs were expected to comprise larger volumes relative to the study's survey.

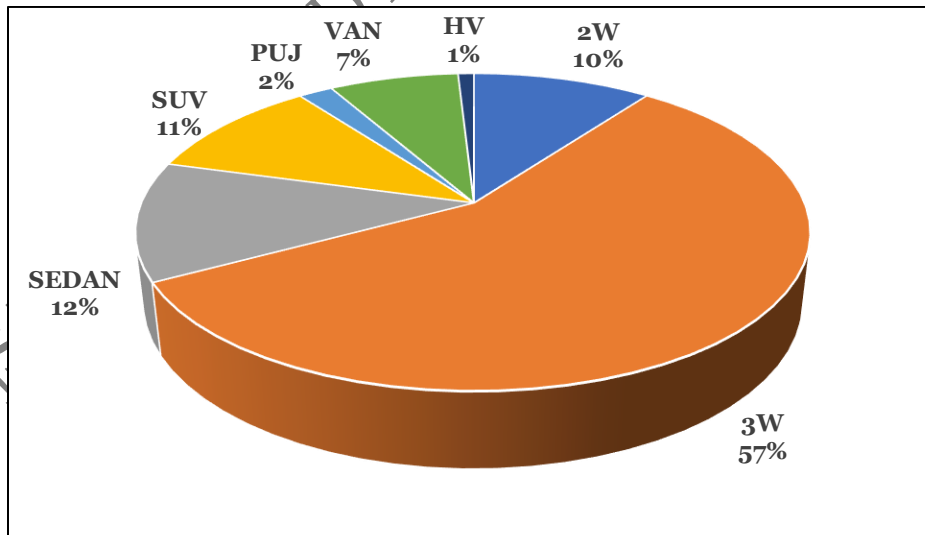


Figure 7. Overall traffic composition from all lane directions.

## Data Extraction and Processing

The peak hour period of 10 to 11 AM was selected based on the traffic volume data, utilizing the passenger car equivalent factors (PCEF) set by the Department of Public Works and Highways (DPWH). To further characterize the chosen peak hour period, the hourly traffic volume per lane direction and the period's traffic composition were determined. Figure 8 shows the traffic volume per lane direction in the selected peak hour period, in which it was determined that the traffic direction of V1 obtained the most traffic flow rate with 1839 pcu/hr. Moreover, Figure 9 summarizes the peak hour period traffic composition. This procedure accounts for the significance of traffic volume in the safety evaluation of unsignalized intersections.

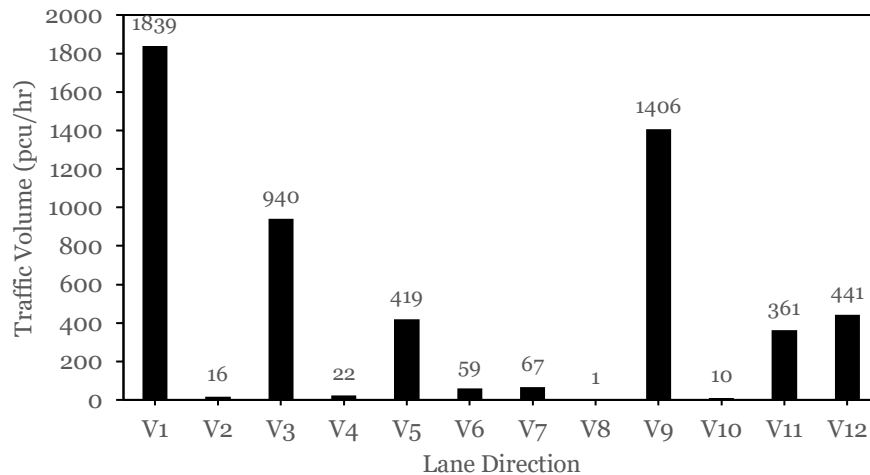


Figure 8. Traffic volume per lane direction within the peak hour period.

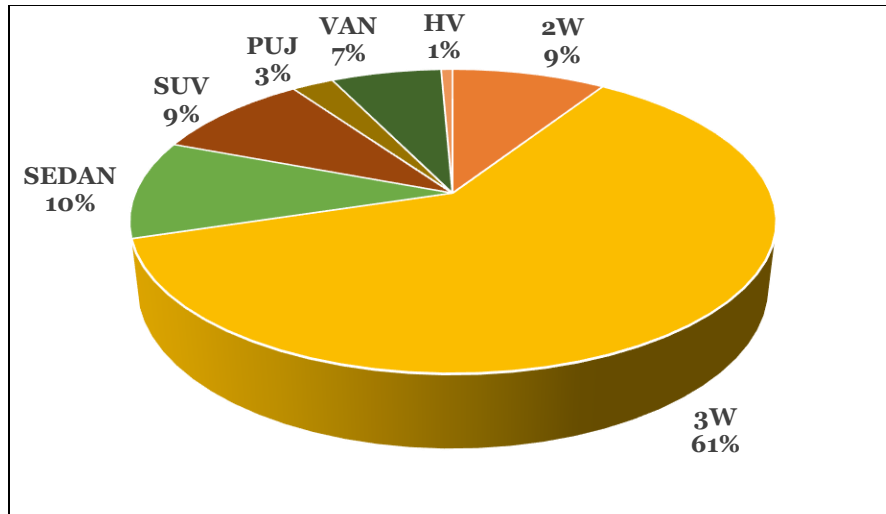


Figure 9. Traffic composition within the peak hour period.

The manual frame counting method was used in processing the peak hour period footage for safety analysis. It involves the determination of conflict zone references for the computation of PET counts. For this study, 2.5 m by 2.5 m grids were overlaid on the study site based on the study Killi and Vedagiri (2014). The study is limited by the footage specifications, wherein the available footages are recorded at a framerate of 24 frames per second (fps). Babu and Vedagiri (2016) measured the PET at a framerate of 25 fps, indicating a PET measurement accuracy of 0.040 s. The study of Killi and Vedagiri (2014), on the other hand, used a playback speed of 6 fps which results to a better accuracy of 0.01 s. Their studies indicate that measuring PET at more precise frame rates provides better accuracy. This is evident through a manual frame counting method since the footage is being analyzed on a frame-by-frame basis. The lower the number of frames being played in a second can show more detailed vehicle movement. Additionally, limitations include measurement error from the differences between the real-life and image space provided by the footage. The scale of these grids was referenced to the map scale available from Google Maps. Through Autodesk AutoCAD, a map-scaled grid was initially overlaid on the top view of the intersection in the study and is presented in Figure 10.



Figure 10. Overview of reference grids on the study site.

After which, the 2.5 m by 2.5 m grid was converted to a footage ratio of 704 by 408 pixels to be superimposed on the video footage. It should be reiterated that the study assumed a procedure that only approximates actual measurements, most particularly on the overlaying of grids on the video footage. The adapted procedure still provides close approximations for the accessibility of PET counts (Ismail et al. 2013; Kassim et al. 2014) even without the use of camera calibration techniques. Overlaid grids on the footage are presented in Figure 11.

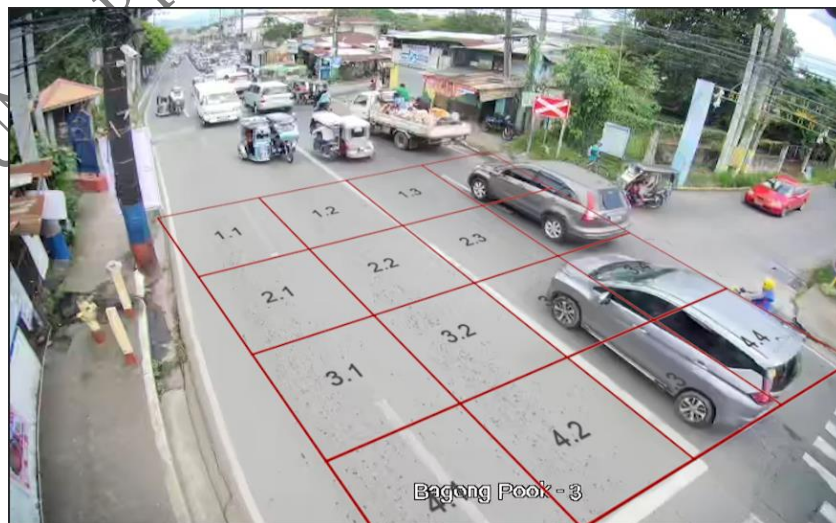


Figure 11. Reference grid layout on the peak hour video footage.

Conflict zones were identified through the grid layout according to their type of turning movement. Each cell within the grid was given an identification number to allow for easier procedures in identifying critical conflict spots. With this, PET counts can then be manually processed through simultaneous observation of the processed footage and encoding of conflict time instances in a dedicated spreadsheet. From the peak hour footage, the traffic conflicts were observed on a frame-by-frame basis. This study focuses on turning conflicts, which is defined by the instance of a vehicle exiting a conflicted spot ( $t_1$ ) and the instance of the next vehicle entering the same conflict spot ( $t_2$ ). PET can then be calculated using equation 1. The equation denotes the time difference between the two observed instances and is represented by a conflict spot. A higher difference between  $t_1$  and  $t_2$  represents a large PET value that depicts a longer time interval before a collision happens between the observed vehicles in these two instances. Large values of PET are usually disregarded in critical conflicts analysis as these pertain to non-hazardous events (Kassim et al., 2014). On the other hand, PET values that are closer to zero are those regarded as traffic conflicts. These also include events where PET values are less than zero, wherein such cases happen when the next vehicle enters before the first vehicle exits it. Numerically, the recorded instance of the first vehicle exiting the conflict spot ( $t_1$ ) will be larger than the recorded instance of the next vehicle entering the conflict spot ( $t_2$ ). By Equation 1, a negative PET will be obtained in this type of event.

$$PET = t_2 - t_1 \quad \text{Eq. 1}$$

This procedure was conducted on every turning movement, particularly, right-turning movement from the minor road, and left-turning movement from both minor and major roads. The type of vehicle involved in an observed traffic conflict was also recorded for statistical analysis.

### **Safety Analysis**

Critical conflicts are analyzed through the determination of critical zones and turning movements of vehicles within the intersection. Since the PET count procedure has also accounted for the location of each conflict instance by providing a dedicated column for conflict zones, the number of recurring conflicts for each conflict zone can then be tallied. The same can be done in obtaining the most critical turning movement, as PET counts were tallied according to it.

Easyfit application has then been used to formulate numerical descriptive measures for the data collected from PET counts. This is to provide parameters for the distribution fitting processes, which would be used in generating calibrated crash frequency prediction models.

After obtaining the normality of the PET count dataset from descriptive statistics, the data is then tested for the best-fitting distribution model via Easyfit. The application uses the tests of Kolmogorov-Smirnov (KS), Anderson-Darling, and Chi-Square Goodness-of-fit (GOF) in finding the most reliable mathematical model for the obtained dataset. These tests are done by following the standard methods of GOF tests, in which the null and alternative hypotheses are evaluated through computed test statistics. Easyfit determines the best-fit model by listing the top distributions that could fit the data according to their computed test statistic. All tests were done in 20%, 10%, 5%, 2%, and 1% levels of significance to determine the minimum range of precision at which a model can fit the data.

In estimating the likelihood of crashes, each distribution uses a corresponding probability density function and various empirical parameters. These empirical parameters are solved by the program through the cumulative probabilities of the actual and theoretical data. Easyfit assumes initial theoretical data that closely fits the actual dataset, and the difference between both datasets is compared. As determined by Easyfit for this study, the distribution models of Johnson SU, Three-Parameter Log-Logistic, and GEV are to be given emphasis.

Johnson SU uses the function presented in equation 2, where  $\gamma$  is the shape parameter 1,  $\delta$  is the shape parameter 2,  $\lambda$  is the scale parameter, and  $\xi$  is the location parameter.

$$f(x) = \frac{\delta}{\lambda\sqrt{2\pi}\sqrt{z^2+1}} \exp\left(-\frac{1}{2}\left(\gamma + \delta \ln(z + \sqrt{z^2 + 1})\right)^2\right) \quad \text{Eq. 2}$$

Equation 3 then presents the function used for the Three-Parameter Log-Logistic model, where  $\alpha$  is the shape parameter,  $\beta$  is the scale parameter, and  $\gamma$  is the location parameter.

$$f(x) = \frac{\alpha}{\beta} \left(\frac{x-\gamma}{\beta}\right)^{\alpha-1} \left(1 + \left(\frac{x-\gamma}{\beta}\right)^\alpha\right)^{-2} \quad \text{Eq. 3}$$

Lastly, the GEV distribution uses the probability density function presented in equation 4, where  $k$  is the shape parameter,  $\sigma$  is the scale parameter,  $\mu$  is the location parameter.

$$f(x) = \begin{cases} \frac{1}{\sigma} \exp\left(-\left(1 + kz\right)^{-\frac{1}{k}}\right) \left(1 + kz\right)^{-1-\frac{1}{k}} & k \neq 0 \\ \frac{1}{\sigma} \exp(-z - \exp(-z)) & k = 0 \end{cases} \quad \text{Eq.4}$$

The best-fitted model aims to predict the probability of a PET value less than or equal to zero, representing the occurrence of a crash. Since this study used the peak hour period for analysis, then the probability of crashes was predicted in hourly intervals. After obtaining the best-fit model



for the data, an annual crash risk frequency estimate can be obtained by using exposure factors. Reddy et al. (2019) estimated crash frequency by associating the occurrence of crashes or traffic conflicts with unit exposure. By following this premise, the probability obtained from the best-fit model can be multiplied to an average exposure time wherein conflicts can happen. This exposure time was assumed to be 12 hours per day or 4380 hours in a year. Equation 5 simplifies this estimation, where  $C$  is the crash frequency per hour in a year, and  $E$  is the average hourly exposure time in a year.

$$C = (\text{Probability of } PET < 0s) \cdot (E) \quad \text{Eq. 5}$$

## RESULTS

### Post-Encroachment Time Data

A sample of recorded data is provided in Table 1, which shows the spreadsheet format for manual PET measurement. The time instances of a first exiting vehicle's rear end touching the edge of a conflict zone are labeled as First Exit ( $t_1$ ), while the events of a last vehicle's front end entering the conflict zone are labeled as Last Entry ( $t_2$ ). Moreover, the frequency of conflicts according to conflict spots was also recorded for critical conflicts analysis.

Table 1. Sample Spreadsheet for Manual PET Measurements in conflict spots.

Conflict ID	Conflict Spot	First Exit (t1)		Last Entry (t2)		PET (s)	Type of Vehicle	
		mm	ss	mm	ss		Turning	Through
1	1.4	0	3.04	0	4.09	1.043	3W	SEDAN
2	1.4	0	4.00	0	4.09	0.083	3W	2W
3	1.4	0	5.80	0	4.09	-1.71	3W	2W
4	1.4	0	7.67	0	5.84	-1.84	3W	VAN
5	1.4	0	21.60	0	21.77	0.17	SEDAN	VAN
6	1.4	0	21.60	0	25.285	3.67	2W	VAN
7	1.4	0	21.60	0	26.11	4.51	3W	VAN
8	1.4	0	21.60	0	29.07	7.47	3W	VAN
9	1.4	0	21.60	0	31.249	9.64	SEDAN	VAN

10	1.4	0	21.60	0	35.20	13.60	3W	VAN
11	1.4	0	37.95	0	36.75	-1.21	3W	3W
12	1.4	1	0.06	1	8.57	8.51	SEDAN	3W
13	1.4	1	15.53	1	16.16	0.63	SEDAN	SUV
14	1.4	1	22.62	1	24.469	1.84	SEDAN	2W
15	1.4	1	30.54	1	29.265	-1.29	3W	3W
16	1.4	1	44.10	1	45.73	1.63	VAN	VAN
17	1.4	1	58.08	1	59.04	0.96	VAN	VAN
18	1.4	2	1.66	2	2.16	0.50	VAN	VAN
19	1.4	2	17.64	2	17.76	0.13	VAN	SEDAN
20	1.4	2	20.775	2	21.10	0.33	PUJ	SEDAN

### Critical Zones Determination

Conflict zone frequencies were tallied according to their type of turning movement. The zones with the highest frequencies of traffic conflict are then deemed critical. Table 2 shows the summary of conflict frequencies according to their conflict zones. The conflict spot of 1.4 obtained the highest number of occurring conflicts with a count of 477. This was followed by conflict spots 3.4 and 2.4, with 310 and 239 conflicts respectively. Moreover, the event of left-turning vehicles from the major road contributed the most in conflict occurrences within the intersection.

Table 2. Summary of Conflicts According to Conflict Zones for turning vehicles.

Conflict Zones	Right-Turning Vehicles from Minor Road	Left-Turning Vehicles from Minor Road	Left-Turning Vehicles from Major Road	Total
1.1	0	0	0	0
1.2	0	4	0	4
1.3	0	0	61	61
1.4	468	2	7	477
2.1	0	3	0	3
2.2	0	9	1	10
2.3	0	29	168	197
3.1	0	20	0	20
3.2	0	25	0	25
3.3	0	55	84	139
3.4	0	55	255	310
4.1	0	2	0	2

4.2	0	22	1	23
4.3	0	8	14	22
4.4	0	0	19	19
Total	473	283	795	1551

## Descriptive Statistics

After processing the PET counts, the resulting dataset was analyzed through descriptive statistics and is presented in Table 3. 16 PET values were obtained, which also describes the total number of turning vehicle conflicts in the intersection throughout the observation period. The mean PET value for the intersection is 3.57s and each observation deviated from the mean by 4.772s on average. At 95% confidence, the average PET value in the intersection lies within 3.33s and 3.81s. The positive skewness value of 2.06 means that there are generally low values of observed PET in the intersection, denoting higher risks for right-angle collisions. The measure of kurtosis also indicated that the data is not normally distributed. To further characterize the dataset, a histogram of the PET count has also been provided in Figure 12.

Table 3. Descriptive Statistics of PET Count Data.

Statistic	Value
Sample Size	1551
Range	60.978
Mean	3.5663
Variance	22.772
Std. Deviation	4.772
Coef. of Variation	1.3381
Std. Error	0.12117
Skewness	2.056
Excess Kurtosis	12.107
Minimum	-26.944
Maximum	34.034

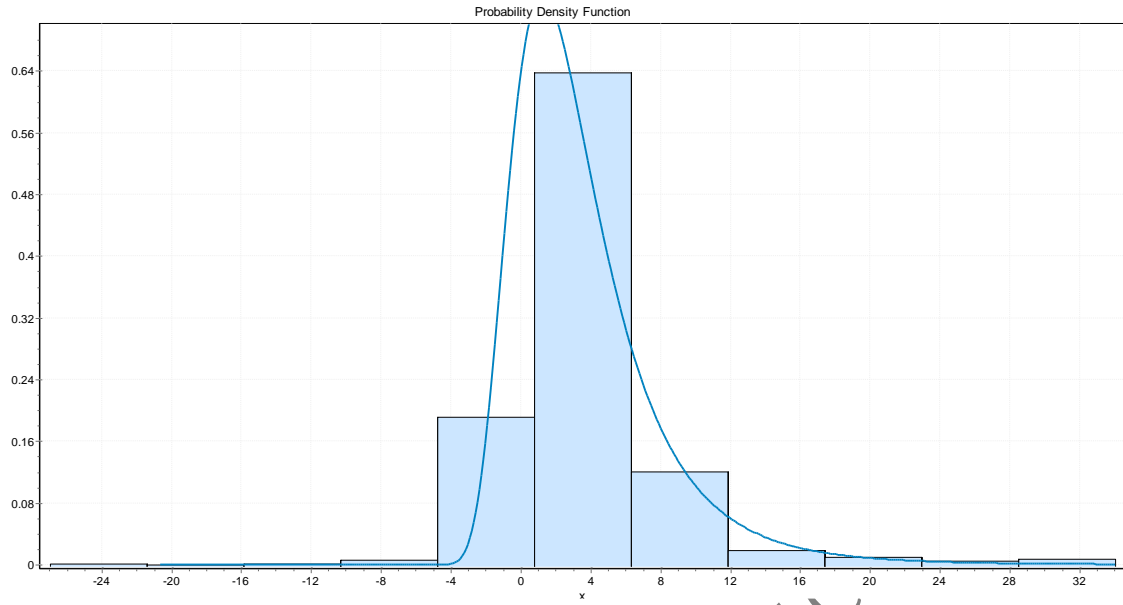


Figure 12. Histogram of PET values.

### Crash Frequency Prediction

Table 4 summarized the results from the different tests for goodness of fit. It is observed that the computed test statistics for all of the tests were higher than the critical values at all levels of significance, hence, the null hypothesis is rejected. The actual data does not follow these distributions; however, these models have the lowest values of test statistics relative to other fitted distributions in Easyfit. The most fitting distribution for the Anderson-Darling test, Kolmogorov-Smirnov test, and Chi-square GOF test are Johnson SU, GEV, and Johnson SU, respectively.

Table 4. Summary of Results from the different tests for goodness of fit.

Type of Test	Distribution	Parameters	Test Statistic	Critical Values ( $\alpha = 0.2, 0.1, 0.05, 0.02, 0.01$ )
Anderson-Darling Test	Johnson SU	$\gamma=-0.92$ $\delta=1.37$ $\lambda=3.82$ $\xi=-0.03$	17.21	1.37, 1.93, 2.50 3.29, 3.91
	Log-Logistic (3P)	$\alpha=18.91$ $\beta=38.42$ $\gamma=-35.45$	19.76	
	Cauchy	$\sigma=1.70$ $\mu=2.38$	36.67	

Kolmogorov-Smirnov Test	General Extreme Value	$k=0.13 \quad \sigma=2.78 \quad \mu=1.58$	0.077	0.03, 0.03, 0.03, 0.04, 0.04
	Log-Logistic (3P)	$\alpha=18.91 \quad \beta=38.42 \quad \gamma=-35.45$	0.08	
	Johnson SU	$\gamma=-0.92 \quad \delta=1.37$ $\lambda=3.82 \quad \xi=-0.03$	0.083	
Chi-square GOF Test	Johnson SU	$\gamma=-0.92 \quad \delta=1.37$ $\lambda=3.89 \quad \xi=-0.032$	123.92	13.44, 15.99, 18.31, 21.16, 23.21
	Log-Logistic (3P)	$\alpha=18.91 \quad \beta=38.42 \quad \gamma=-35.45$	192.81	
	Cauchy	$\sigma=1.70 \quad \mu=2.38$	271.87	

The top three distributions from the different fitting tests were used for the comparison of probability functions for crash risk estimation in which the Johnson SU function was found to be the most like the PET histogram. Additionally, it has also been consistently ranked as the topmost model in the GOF tests.

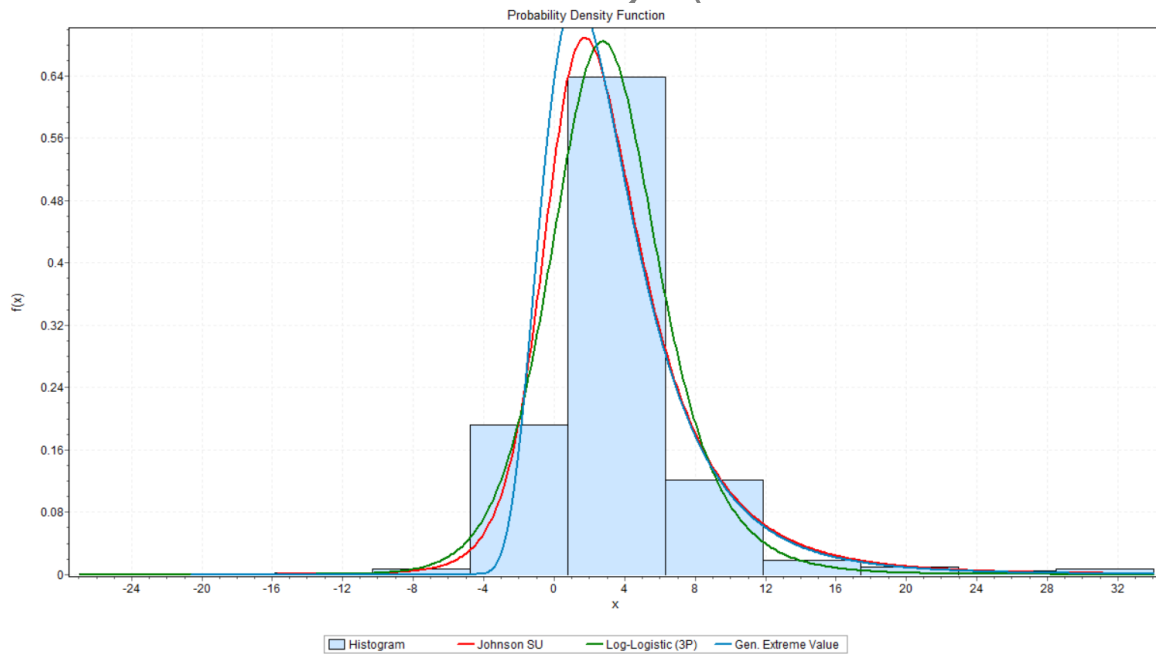


Figure 13. The fit of PET values using GEV, Log-Logistic, and Johnson SU distributions.

Through Equation 2, the probability distribution curve of Johnson SU has been obtained and its parameters are evaluated in Table 5.

Table 5. Johnson SU Parameter Values

Probability Distribution Curve	Parameter	Value
Johnson SU	$\gamma$	-0.92
	$\delta$	1.37
	$\lambda$	3.82
	$\xi$	-0.03
Log-Logistic	$\alpha$	18.91
	$\beta$	38.42
	$\gamma$	35.45
GEV	$k$	0.13
	$\sigma$	2.78
	$\mu$	1.58

By using the probability density function obtained from Johnson SU, the probability of vehicular crash events can be estimated. The probability is computed through the fitted distribution profile and is estimated to be 18.11%. It could then be predicted through Equation 5 that 793 crashes per hour can occur each year.

## DISCUSSION

Statistical modeling procedures have then found that the top three fitting distributions for the PET dataset are Johnson SU, three-parameter Log-Logistic, and GEV models. The resulting estimations from these distributions show that the three-parameter log-logistic and GEV models tend to estimate lower prediction values; hence, the Johnson SU model was chosen as the best-fit model for crash frequency estimation. Using this model, it was found that the probability of right-angle crashes within the intersection is 18.11%. This probability also pertains to a prediction of 793 right-angle crashes per year. Given these estimations, it can be said that the unsignalized three-legged intersection in this study is at relatively lower crash frequency rates as compared to the study conducted by Pawar et al. (2018), in which an undivided unsignalized intersection has

obtained an overall estimate of 30% probability of a crash. It was also observed that the resulting estimate from this study is lower than the divided intersection variant in the study of Pawar et al., which obtained a value of 21% probability of crash estimate. It was concluded from their study that divided intersections have lower estimates of crashes due to an improved driving environment (Pawar et al. 2018). The results from this study deviated from their conclusions for divided unsignalized intersections. Moreover, Reddy et al. (2019) have conducted the same methodology on an uncontrolled four-legged intersection to determine the reduction of crash risk induced by the installation of speed bumps within the intersection. It was observed from their study that the annual crash frequency was 437 crashes per year at the base case of the intersection, which is significantly lower than the obtained estimate in this study. For the case of controlled four-legged intersections, Songchitruska (2004) has conducted studies on 18 intersections with the same controlled configurations, in which the standard annual crashes count of 2.8302 and 3.7910 at 85th and 90th percentiles, have been established respectively. It should be noted that the counts for controlled intersections deviate significantly from uncontrolled crash estimates.

The results from previous literature imply that the difference in driving environments and intersection configurations are to be considered when comparing safety evaluation studies using the procedure of proximal surrogate analysis. Moreover, crash frequency counts from previous works are relative to the respective traffic environment in which their studies were done. In order to achieve an accurate comparative analysis of crash frequencies, the reference traffic environment must be identical. Due to this limitation, concluding if the intersection is safe or unsafe is still considered unachievable. As stated by Zheng et al. (2014), it could be established that difficulties in the cross-validation and generalization of results are still common in this method due to the shortage of standards for researchers to base their comparisons. However, the safety evaluations

for this intersection still stand with the obtained crash risk estimates. This study provided the current safety parameters of the intersection, and additional research is needed to establish standards for developing intersection safety thresholds. These safety parameters allow the evaluation of potential road geometry changes, traffic management policies, and other safety mitigation procedures that could affect the risk of transverse collisions within the intersection. Furthermore, supplementary studies for the variables presented in the obtained PET dataset can also be pursued.

## **ACKNOWLEDGEMENT**

The researchers would like to thank the San Pablo City Traffic Management Office for providing the traffic video footage that was used in this study. Without the support and data provided, this study would not have been completed.

## **REFERENCES**

- Babu S and Vedagiri P. 2018. Proactive safety evaluation of a multilane unsignalized intersection using surrogate measures. *Transportation Letters*. 10(2): 104-112. DOI: 10.1080/19427867.2016.1230172
- Chin H and Quek S. 1997. Measurement of traffic conflicts. *Safety Science*. 26(3): 169-185. DOI: 10.1016/S0925-7535(97)00041-6
- Farah H and Azevedo C. 2017. Safety analysis of passing maneuvers using extreme value theory. *IATSS Research*. 41(1): 12-21. DOI: 10.1016/j.iatssr.2016.07.001
- Glauz W and Migletz DJ. 1980. Application of traffic conflict analysis at intersections. National Cooperative Highway Research Program Report, Kansas City, Missouri. 118pp.



[http://onlinepubs.trb.org/Onlinepubs/nchrp/nchrp\\_rpt\\_219.pdf](http://onlinepubs.trb.org/Onlinepubs/nchrp/nchrp_rpt_219.pdf). Accessed on 10 January 2021.

Goyani J, Nishant P, Gore N, Jain M and Arkatkar S. 2019. Investigation of traffic conflicts at unsignalized intersection for reckoning crash probability under mixed traffic conditions. *Journal of the Eastern Asia Society for Transportation Studies*, 13: 2091-2110. DOI: 10.11175/easts.13.2091

Hyden C. 1987. The development of a method for traffic safety evaluation: The Swedish Traffic Conflicts Technique. Lund, Sweden. 57pp.

Ismail K, Sayed T and Saunier N. 2013. A methodology for precise camera calibration for data collection applications in urban traffic scenes. *Canadian Journal of Civil Engineering*. 40(1): 57-67. DOI: 10.1139/cjce-2011-0456

Kassim A, Ismail K and Hassan Y. 2014. Automated measuring of cyclist – motor vehicle post encroachment time at signalized intersections. *Canadian Journal of Civil Engineering*. 41(7): 605-614. DOI: 10.1139/cjce-2013-0565

Killi D and Vedagiri P. 2014. Proactive evaluation of traffic safety at an unsignalized intersection using micro-simulation. *Journal of Traffic and Logistics Engineering*. 2(2): 140-145. DOI: 10.12720/jtle.2.2.140-145

Mahmud S, Ferreira L, Hoque M and Tavassoli A. 2016. Application of proximal surrogate indicators for safety evaluation: a review of recent developments and research needs. *IATSS Research*. 41(4): 153-163. DOI: 10.1016/j.iatssr.2017.02.001

MMDA-TEC-Road Safety Unit. 2019. MMARAS annual report. TEC-Road Safety Unit. 24pp.  
[https://mmda.gov.ph/images/Home/FOI/MMARAS/MMARAS\\_Annual\\_Report\\_2019.pdf](https://mmda.gov.ph/images/Home/FOI/MMARAS/MMARAS_Annual_Report_2019.pdf)

f. Accessed on 12 October 2020.

Parker Jr. M and Zegeer C. 1989. Traffic Conflict Techniques for Safety and Operations. Observers Manual. Wayne, Michigan. 40pp.

<https://www.fhwa.dot.gov/publications/research/safety/88027/88027.pdf>. Accessed on 10 January 2021.

Pawar N, Gore N and Arkatkar S. 2018. Influence of driving environment on safety at unsignalized t-intersection under mixed traffic conditions. In: Deb D, Balas VE, Dey R and Shah J (eds). Innovative Research in Transportation Infrastructure, pp. 23-31.

PhilAtlas (2023). San Pablo Province of Laguna. Accessed at <https://www.philatlas.com/luzon/04a/laguna/san-pablo.html>

Pirdavani A, Brijs T, Bellemans T and Wets G. 2010. Evaluation of traffic safety at unsignalized intersections using microsimulation: a utilization of proximal safety indicators. Advances in Transportation Studies: an International Journal Section, 22.

Reddy SK, Chepuri A, Arkatkar S and Joshi G. 2019. Developing proximal safety indicators for assessment of un-signalized intersection: A Case Study in Surat City. Transportation Letters. 12(5): 303-315. DOI: 10.1080/19427867.2019.1589162

Songchitruska P. 2004. Innovative non-crash-based safety estimation: An Extreme Value Theory Approach. Doctor of Philosophy. Purdue University-West Lafayette, Indiana, United States of America. 368pp.

Varlhelyi A, Laureshyn A and Johnsson C. 2018. Surrogate measures of safety and traffic conflict observations. In: Polders E and Brijs T (eds). How to Analyse Accident Causation: A Handbook with Focus on Vulnerable Road Users, pp. 95-128.

World Health Organization. 2018. Global Road Safety Status. 424pp. [https://www.who.int/violence\\_injury\\_prevention/road\\_safety\\_status/2018/en/](https://www.who.int/violence_injury_prevention/road_safety_status/2018/en/). Accessed on 12 October 2020.

Zheng L, Ismail K and Meng K. 2014. Traffic conflict techniques for road safety: analysis open questions and some insights. Canadian Journal of Civil Engineering. 41(7): 633-641. DOI: 10.1139/cjce-2013-0558

CMUJS UNCORRECTED PROOF ARTICLE CONFIDENTIAL